Flood Vulnerability Assessment of Urban Traditional Buildings in Kuala Lumpur, Malaysia

Dina D'Ayala[1*], Kai Wang[1], Yuan Yan[1], Helen Smith[2], Ashleigh Massam[2], Valeriya Filipova[2],
Joy Jacqueline Pereira[3]

1. *Epicentre Research Group, Department of Civil, Environmental and Geomatic Engineering, University College London, UK*
2. *JBA Risk Management, Skipton, UK*
3. *Southeast Asia Disaster Prevention Research Initiative (SEADPRI), Institute for Environment & Development (LESTARI), Universiti Kebangsaan Malaysia, Malaysia*

Corresponding author: Dina D'Ayala, d.dayala@ucl.ac.uk

Abstract: Flood hazard is increasing in frequency and magnitude in Southeast Asia major metropolitan areas due to the effects of fast urban development and changes in climate, threatening people's properties and life. Typically, flood management actions are mostly focused on large scale defenses, such as river embankments or discharge channels or tunnels. However, these are difficult to implement in historic centres without disturbing their heritage value, and might not provide sufficient mitigation in these areas. Therefore urban heritage buildings may be particularly exposed to flood events, even when they were originally designed and built with intrinsic resilient measures, based on the local knowledge of the natural environment and its threats at the time. Their attractiveness, cultural and economic values, means that they can represent a proportionally high contribution to losses of any event. Hence it is worth to pursue more localised, tailored, mitigation measures.

 Vulnerability assessment studies are essential to inform the feasibility and development of such strategies. In the present paper we propose a multi-level methodology to assess the flood vulnerability of residential buildings in an area of Kuala Lumpur Malaysia characterised by traditional timber housing. The multi-scale flood vulnerability model is based on a wide range of parameters, covering building specific parameters, neighbourhood conditions and catchment area condition. Parameters for 163 buildings were measured in detail by a field surveys integrated with Google Street View. The vulnerability model is combined with high resolution fluvial and pluvial flood maps providing likely water depths for a range of different flood return periods. The obtained vulnerability index shows ability to reflect different exposure by different building types and their relative locations. The study provides evidence that results obtained for a small district can be scaled up at city level, to inform both generic and specific protection strategies. The paper discusses these in relation to a scenario event of 0.1% Annual Exceedance Probability (AEP), based on hydrological and hydraulic models developed for the Disaster Resilient Cities Project.

1. Introduction

The Sendai Framework 2015- 2030 identifies clearly both climate change and rapid urbanisation as disaster risk drivers (UNISDR, 2015). Temperature rise and global warming are strictly correlated to increased rainfall (Wang et al., 2017; Min et al., 2011) and in turn with the increased frequency and
40   extent of droughts and floods (IPCC, 2013, 2014; Mysiak et al., 2016; Pall et al., 2011). Flood risk however is compounded not only by intensified hazard, but very importantly also by increased exposure due to increased urbanisation along coastlines, river basins and flood plains (Kundzewicz et al., 2014; Neumann et al., 2015). Such flood risk become even more challenging in the South and Southeast Asia, as observed (Najibi and Devineni, 2018) and projected (Hirabayashi et al., 2013) flood frequency show
45   dramatic increasing trends.

Following studies on the increased flood risk caused by the increasing rate of impervious surface to drainage capacity in urban areas, (e.g. Ashley et al., 2005; Jacobson, 2011; Jha et al., 2012; Liao, 2012), the shift from control to adaptation in urban flood resilience is increasingly advocated by governmental agencies, experts and developers alike. Mitigating structural measures have the objective of reducing
50   the hazard, i.e. the runoff, by diverting it and channel it. However, structural measures are mostly planned at the large scale, require large investments, long implementation periods, extensive socio-political negotiation. As a consequence of the long timeframe, they might turn out to be inadequate, postponed or irreversible (Aerts et al., 2014), and in many cases they prove to be unsuitable for developing countries on economic and financial grounds (Inaoka et al., 2019). Non-structural measures,
55   however, can provide faster flood risk mitigation, yielding improved adaptability, more distributed benefits and, as a result, better governance (Tullos, 2018; Roslan et al., 2019).

Studies specific to Malaysia have shown that rapidly increasing flood events in recent decades are due to unrestrained occupation of rivers by human activities, destruction of forest and extreme weather events caused by climate change (Aliagha et al., 2015). Statistics show an average of 143 floods per
60   year since 2001, of which more than 90% are flash floods (Mohd Anip and Osman, 2017). Such frequently occurring floods cause a high level of threat to Malaysian citizens' personal safety and property, thereby, inflicting considerable damage to the country's infrastructure (Nasiri and Shahmohammadi-Kalalagh, 2013). Data from the UNDRR's Country Disaster and Risk Profile (PreventionWeb, 2019) shows for Malaysia that floods account for 98% of average annual loss in the
65   period 1990 to 2014. A report from the Malaysian Department of Irrigation and Drainage, identified an average of 29,000 sq.km or 9% of the country's total land area and more than 4.82 million people (22% of the population) as affected by flooding every year. The annual losses were evaluated at RM915 million (CFE-DMHA, 2019; Nasiri and Shahmohammadi-Kalalagh, 2013). At the beginning of the millennium an integrated flood management strategy was launched, whereby the Malaysian government
70   invested in some major structural measures, along with non-structural measures and community

participation (KTA Tenaga Sdn. Bhd., 2003). In terms of urban flood mitigation, among the structural measures, the most conspicuous intervention was certainly the SMART project, Stormwater Management and Road Tunnel, aim at alleviating the flooding problem in the City Centre of Kuala Lumpur caused by the Klang River, as well as reducing traffic congestion (Abdullah, 2004). Among 75 the non-structural measures the government invested in flood detection and warning systems, awareness campaigns and flood proofing guidelines for buildings with basement (DID, 2006, 2008).

Notwithstanding this proactive approach, the "Malaysia Disaster Management Reference Handbook 2019", (CFE-DMHA, 2019) states that: "Annually, floods account for the most frequent and significant damage, with 38 damaging events in the last 20 years, and are responsible for a significant number of 80 human lives lost, disease epidemics, property and crop damage, and other losses". The Handbook also points out that risk of floods has increased due to climate change and that "Malaysia had the highest percentage of the population (67%) exposed to floods among ASEAN (Association of Southeast Asian Nations) member states between July 2012 and January 2019". With six major events in the last five years, flooding remains a major source of risk and losses in Malaysia, with a dramatic three-fold 85 increase of population exposure in two decades. While the Malaysian government has officially adopted a holistic approach to flood risk reduction from preparedness to post event relief, its implementation has received critical reviews by several researchers (Shafiai and Khalid, 2016).

Flood vulnerability, refers to the susceptibility of goods and people in any region to suffer damage and losses. An accurate assessment of such vulnerabilities is essential to devise effective flood risk 90 management (Rehman et al., 2019). Vulnerability assessment studies, focusing on different scales (Kundzewicz et al., 2019) and different dimensions (Rehman et al., 2019), have demonstrated the capability of predicting socio-economical damage and risk by floods. In an urban context, flood vulnerability assessment of individual buildings, and the management of the associated risk, has also proven to be an effective way to increase the flood resilience of the whole city (Aerts et al., 2014). Two 95 approaches are common in flood vulnerability assessment, the physical approach and empirical approach (Balica et al., 2013). Physical approaches use hydrological models to estimate the flood hazard and compute economic consequences for a particular event or area on the basis of a damage index relating a measure of intensity of the flood to the associated economic loss. Parametric approaches use a set of quantitative or qualitative indicators to rate the vulnerability of a building or area, with no 100 particular reference to the hazard intensity.

In the present study, the flood risk to residential buildings in Kuala Lumpur, identified by several studies as one of the major contributors to disaster losses in Malaysia (Bhuiyan et al., 2018), is studied by adopting a hybrid approach using a hydrological model to determine the flood hazard and a set of indicators to determine the vulnerability of individual buildings. However, the present model does not 105 compute the mechanical response of the envelop to the water pressure (Custer and Nishijima, 2015).

To determine the actual risk of different types of flooding, fluvial and pluvial, the present study uses a multi-scale approach to assess the vulnerability of traditional houses in Kampung Baru (Figure 1), thus providing evidence to suggest appropriate mitigation strategies at individual building, local compound and catchment scale. The empirical vulnerability model used is particularly suitable for studies at the

110 micro to meso scale levels, aiming at identifying effective non-structural mitigation measures. It relies on a number of quantifiable and qualitative parameters which allow to identify a number of construction typologies typical of the district, with diverse vulnerability level. The local elevation around the building site and its position with respect to any river courses are also surveyed. By conducting on site and virtual surveys the parameters that influence vulnerability can be determined and quantified, and

115 the economic losses due to flood hazards under different return period can be estimated, allowing to produce mappings which identify a ranking of risk at the building and district scale, for a given hazard magnitude. The hazard magnitudes used are water depths, calculated by developing 2D hydrodynamic models to simulate the behaviour of water conveyed by overland flow and river systems in response to rainfall events of different frequencies and intensities. Finally, possible mitigation strategies to the flood

120 risk will be proposed to increase the resilience of residential buildings in the study area, and other Asian regions with the similar climate.

Figure 1: Pluvial Flood in Kampung Baru, 1st October 2019. Due to poor drainage, water depth of 1 meter was reached after 2 hours of rain. (BERNAMA, 2019)

125

2. Data and Methods

2.1 Study Area

The Kampung Baru district is located in the central area of Kuala Lumpur enclosed between the Klang River on the south east and the Sungai Bunus on the north-west (Figure 2(a)). Kampung Baru is an

130 historic Malay Agricultural Settlement dating back more than 100 years, spread over 100 hectares and home to approximately 19,000 residents. While having witnessed the development of the city, and being

currently under pressure of redevelopment, this area still contains a unique building style, retaining the characteristics of both Malay traditional architecture and the ethnic Malay lifestyle. Given its setting, Kampung Baru is prone to both river flooding and flash floods, partly due to the poor drainage system

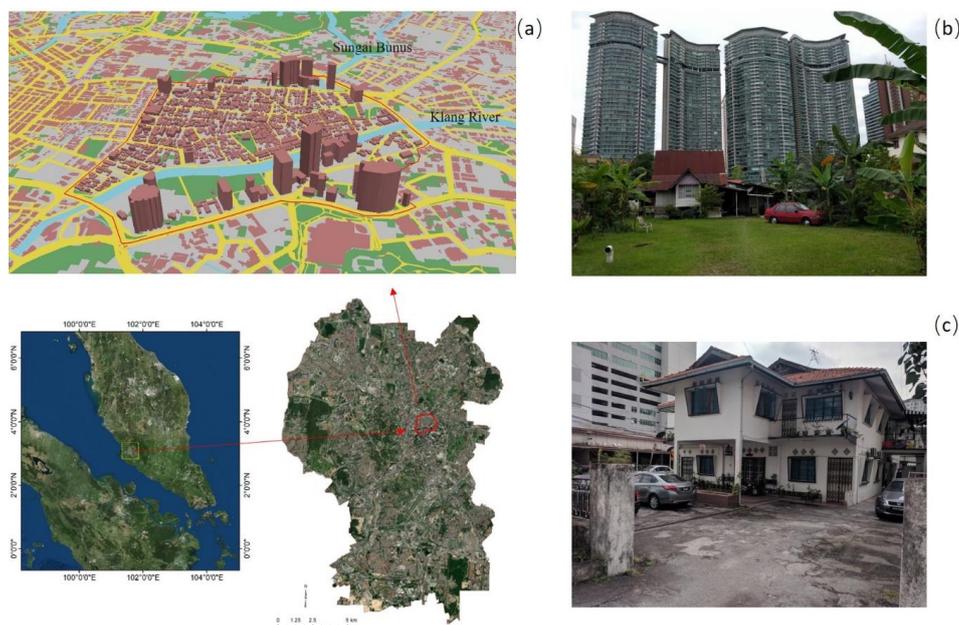135 (BERNAMA, 2019; MENON, 2009) (see Figure 2).

Figure 2: (a) Location of Kampung Baru in the centre of Kuala Lumpur (ESRI ArcGIS® Base Map); (b) traditional Vernacular House; (c) Modern Vernacular House.

140 Ju et al. (2012) recorded 121 traditional vernacular Malay houses, still inhabited by Malay people, in Kampung Baru area. These represent an important cultural and architectural heritage as well as being a touristic attraction and hence representing an important economic resource to the Malay Corporation. Although these houses might have been altered in time, in terms of materials and form, they still maintain two substantial characteristics related to the local environmental conditions: steep sloping roof

145 and floor raised on stilts (Figure 2(b)). These two iconic design features protect the space within from high intensity precipitation and frequent flooding, rendering these houses intrinsically resilient to Malay climate.

Examples of building on stilts in the area of study are shown in Figure 3. Earlier constructions are characterised by buildings on short timber stilts (3a). In some cases, the space below is enclosed by

150 timber grids (3b). In wealthier construction, the stilts might have been made of stone (3c) and in modern construction the stilts have been transformed in ground floor soft storey (3d) to accommodate

carparking, endorsed by the Department for Irrigation and Drainage Malaysia as a non-structural flood mitigation measure.

Figure 3: Typical buildings with stilts, (a) and (b) are more traditional buildings while (c) and (d) are modernized

2.2 Flood hazard mapping

Hazard maps showing flood extent and water depth associated with different types of flooding across Kuala Lumpur were developed within the project for a range of return periods. The maps provide water depth for pluvial flooding (also known as flash flood) and for fluvial (riverine) flooding. For fluvial flooding, two scenarios are mapped: an undefended scenario where no mitigation measures (river flood defences) are accounted for, and a scenario where the flood protection offered by SMART is incorporated.

The maps were developed by analysing time series data from a selection of rain and river gauges across the Klang Basin to calculate design rainfall hyetographs and river hydrographs for return periods of 20, 50, 100 and 200-years. The design rainfall and river flows were used as input for 2D hydraulic modelling using JBA's proprietary JFlow® software (Lamb et al., 2009) to give estimated depths of inundation. The methods used to calculate the rainfall hyetographs and river hydrographs are described in section 2.2.1. An important input to the flood mapping process is a digital terrain model (DTM). For this study, a 0.5m resolution bare-earth DTM was provided by the Civil Engineering and Urban Transportation Department, KL City Hall and City Planning Department, resampled to 5m resolution.

JFlow can be run in different configurations for different purposes. For large rivers, a fluvial model configuration is used to apply hydrographs to the model at regularly spaced inflow points along the

Natural Hazards
and Earth System
Sciences
Discussions

Open Access

EGU

drainage network. The volume of water that can be held within the river channel is estimated and

175   removed from the flood simulation. A JFlow simulation is run for each return period using a solver based upon the two-dimensional Shallow Water Equations. For the SMART scenario a discharge-limited directional culvert is constructed in the JFlow model, to represent the diversion and storage of flood water between Kampung Berembang and the Desa Lake at Salak South, and is adjusted for each of the four SMART operational modes as explained in Table 1.

180   Table 1: Parameters of four SMART operational modes

SMART Mode	Weather condition	Flow at stream gauge L4*	Flow diversion method	Road tunnel status	JBA return period map representing this scenario
1	Fair	< 70m^3/s	N/a	Open to traffic	RP20-RP200 undefended
2	Moderate rainfall	70-150m^3/s	Via lower drains only	Open to traffic	RP20 defended and RP50 defended
3	Major storm	>150m^3/s	Via lower drains and possibly road tunnel	Closed to traffic	N/a
4	Prolonged heavy rain	>150m^3/s and Mode 3 in operation for over 1 hour	Via lower drains and road tunnel	Closed to traffic	RP100 defended and RP200 defended

*L4 gauge is situated at confluence of Upper Klang and Ampang rivers.

For small rivers and pluvial flooding, a direct-rainfall configuration is used. This approach applies the relevant hyetographs to each cell of the DTM. Different runoff and drainage rates are applied to reflect spatial variations in soil type and land cover. Urban drainage systems are accounted for by removing a

185   proportion of the total rainfall volume prior to running the JFlow simulation. Water depth in metres is calculated for each flood type (pluvial, fluvial, and fluvial with SMART defence) and return period (20, 50, 100-year) and recorded in a set of GeoTIFF rasters for use in Geographical Information Systems (GIS). In this study, flood maps of three flood types under 100-year return period are used in the estimation and flood hazard and risk, as is widely used in the communication and decision in flood risk

190   prevention and management.

2.2.1   Calculation of rainfall hyetographs and river hydrographs

Rainfall totals (in mm) were calculated at 11 rain gauge stations within a 6km radius of the centre of Kuala Lumpur. This was done by extracting peak-over-threshold values from the hourly rainfall record at each gauge and fitting them to a Generalised Pareto Distribution, to enable return period rainfall totals

195   to be estimated for each gauge. This was done separately for the 1-hour, 3-hour and 24-hour storm
        durations. Spatial interpolation was then used to convert the estimates at the gauge stations into a set of
        continuous rainfall surface rasters across the entire study area, providing a rainfall total (mm) for each
        return period and storm duration on a 110m x 110m grid. Each gridded rainfall total was converted into
        a hyetograph to describe the temporal distribution of the rainfall for each of the three storm durations.

200   Normalised rainfall profiles were developed by analysing hourly rainfall data for 20 events between
        1997 and 2016 and calculating a mean 3-hr storm profile and a mean 24-hour storm profile across all
        stations. Due to the lack of sub-hourly rainfall data, the 1-hour storm profile was assumed to be a simple
        triangular shape. The storm profiles are illustrated in Figure 4(a) below.
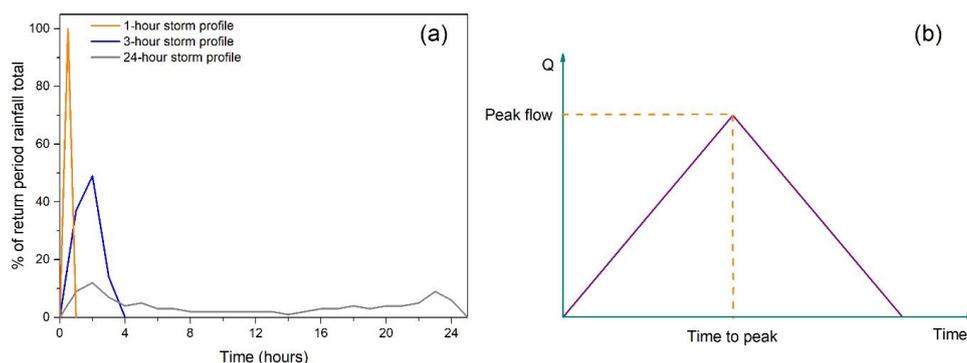
205   Figure 4: (a) Storm profiles used in current flood modelling (b) Schematic diagram of the river
        hydrograph shape

        River hydrographs were calculated at 2km intervals along river network of the study area. Each
        hydrograph was constructed using a linear function, defined by peak flow and time to peak estimates.
        More advanced methods for deriving the shape of hydrographs are available, but in all but exceptionally

210   flat topographies peak flow can be considered the key variable in hydrograph shape, so for this study a
        generalised triangular profile was considered appropriate. Firstly, peak flow was calculated at 10
        streamflow gauges within the Klang River basin, using non-stationary flood frequency analysis. These
        values were then regionalised using a linear regression equation for each return period, enabling peak
        flow to be estimated at all ungauged locations within the study area, based on their catchment area (in

215   km^2).

        The time to peak at each gauge was calculated by extracting the median time to peak from all discrete
        flood events recorded at the 7 streamflow gauges with hourly flow records available. A linear regression
        equation was used to estimate time to peak at all ungauged locations within the study area, which
        correlated time to peak (hours) to catchment area (km^2). Figure 4(b) shows a schematic diagram of the

220   river hydrograph shape.

2.3 Data Collection

Given the multiscale approach adopted for the assessment of the flood risk in Kampung Baru, data is obtained from multiple sources. A 3D building dataset and 0.5-meter resolution DEM dataset were provided by UKM Southeast Asia Disaster Prevention Research Initiative (based on the 2013 LiDAR dataset from the KL City Hall). These have been visualised in ArcMap 10.3 and manipulated to extract data on building's position, footprint, position of the building's plinth relative to the road. This information is essential to determine the depth of water at a particular building perimeter, given a flood depth at the site. Other data were collected from a field survey and Google Street View. A preliminary overview of all buildings in the targeted area of Kampung Baru was completed on Google Street View (GSV), to identify the most interesting sector in the district and proceed to an initial screening of the buildings' typologies present and the identification of critical parameter to best target the field survey. The field survey of Kampung Baru, was conducted in July 2018, to gather specific data relative to individual buildings. Critical parameters, difficult to identify from the GSV, such as the location and dimensions of the drainage system, were typologically classified and measured on site, along with other geometric parameters. A thorough photographic survey was also conducted at this stage, taking shots for all visible and accessible elevations of sample buildings, as well as larger overview shots of the whole study area. Specific features aimed at mitigating flood damage were also observed and recorded during the field survey.

After detailed data was taken on a small sample of buildings during the field survey which also allowed for identification of buildings' typologies, a further survey based on Google Street View (GSV) was undertaken to gather additional data and cover a sample of buildings in excess of 163. This procedure was successfully used by one of the authors to survey buildings to determine vulnerability and damage in post-earthquake reconnaissance (Stone et al., 2017; Stone et al., 2018), and it is increasingly used to produce exposure databases in an expedient and economic manner (Pittore et al., 2018). In GSV, a continuous series of 360-degree panoramas, created by sewing multiple overlapping photos together to display the real portrayal of a specific location, were observed according to the location and the time of when the photos were captured. In Kampung Baru images were collated in three different years of survey, 2013, 2015 and 2017. In this study the latest version was chosen, and a full front sight of a target building could be accessed online through the observation points allocated on each street. During the survey, the qualitative parameters were collected visually as for the field survey. For quantifying the other parameters, such as the height of door threshold and window sills, measured samples from the field survey were used as a reference to apply a measure of scale.

2.4 Vulnerability Model

Research on flood vulnerability and risk assessment encompasses a wide range of methods and focuses (Rehman et al., 2019). In an urban context a substantial component of losses is ascribable to physical

damage to vulnerable buildings and their contents (Chen et al., 2016). Current flood risk assessment study and damage models use either an empirical approach, relying on post event damage data collection to determine vulnerability functions, or synthetic approaches, whereby the vulnerability functions are based on expert opinion. Empirical methods are basin or catchment specific (Merz et al.,

260 2010), hence of limited transferability and applicability to other locations without substantial calibration. Synthetic models are more adaptable spatially and temporally; however, they are often based on a single variable relating flood depth to economic loss, possibly mediated by building type. Dottori et al (2016) present one of the few synthetic flood damage models based on a component-by-component analysis of direct damage, correlating each damage component to different flood actions and specific building

265 characteristics. The damage functions are designed using an expert-based approach validated on loss adjustment studies, and damage surveys carried out for past flood events. Historic data on flood damage and insured losses is not available for Kuala Lumpur or Kampung Baru. It is increasingly recognised that models need to account for multiscale, from single asset to full catchment area, and be able to consider many variables, in terms of both hazard intensity and asset response (Amadio et al., 2019).

270 Such models may rely on sophisticated physical modelling of the flood event, while hazard-damage correlations are then determined using artificial neural networks or random forests analysis of past damage data (e.g. Carisi et al., 2018;Merz et al., 2013), or Bayesian networks (Vogel et al., 2014). For the majority of these models, however, while hazard and exposure are treated to a high level of resolution, the individual building's vulnerability descriptors are limited in number and often of a

275 qualitative nature. Although Custer and Nishijima (2015), Herbert et al. (2018), Kelman and Spence (2003) and Milanesi et al. (2018) have used mechanical approaches to determine the structural capacity of individual masonry walls to water pressure and derive vulnerability functions which correlate physical damage to depth of water, such physical models have not so far found direct application at urban scale.

280 In the present study, a vulnerability index approach is applied to determine the relative vulnerability of individual buildings. The vulnerability index is obtained by identifying a number of parameters which are considered specifically representative of the local setting, ranging from building characteristics to surrounding conditions. The parameters used in the present study for characterising the building vulnerability are adapted from studies conducted by one of the authors on historic buildings in UK

285 (Stephenson and D'Ayala, 2014) and the Philippines (D'Ayala et al., 2016). To these a classification of drainage conditions and relative position of the building to local topography and relative position to waterways are added. The full list of parameters is illustrated in Figure 5 and Table 2. The attributes for each parameter and the rating scheme adopted are further described in the next section.
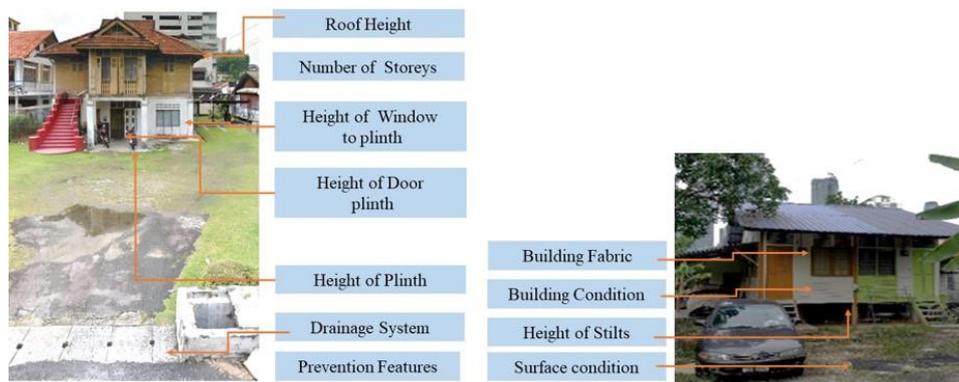
290   Figure 5: Example of traditional buildings in Kampong Baru and indication of the vulnerability index
parameters

Table 2: Flood Vulnerability Index parameters.

PARAMETER	DESCRIPTION	UNITS
1. Number of storeys	Maximum number of storeys of the building	-
2. Footprint	Building Footprint area at ground floor	m^2
3. Height of plinth	Height of the plinth relative to the road	m
4. Height of Stilts	Stilt height over building plinth	m
5. Height of door	Height of door threshold to the plinth	m
6. Height of window	Height of window sill to the plinth	m
7. Building fabric	Structure and cladding material	-
8. Building condition	The level of maintenance and building quality	-
9. Drainage system	The level of drainage system around the building	-
10. Surface condition	Type of surface around the building, surface cover, inclination and permeability	-
11. Prevention features	The measures of flood prevention for the target building	-

295   **2.5 Vulnerability Ratings**

For each parameter a range of attributes varying between 3 and 5 was determined through logical derivation of the maximum possible number of responses and these were assigned a vulnerability rating (VR) on a scale from 10 to 100. The scale is divided into equal, unweighted parts according to the number of attributes, with the attribute indicating lowest vulnerability assigned the value 10, and the

300   one indicating the highest assigned the value 100, as shown in Table 2, following the PARNASSUS

V.1 procedure (Stephenson and D'Ayala, 2014). For instance, the parameter 'drainage system' has three possible outcomes: 'good', 'poor' and 'no', so that the numerical rating among these three outcomes can be assigned as 10, 55 and 100, to represent the increase in vulnerability. Table 3 summarise each parameter range of attributes and its conversion into vulnerability rating. The surface condition consists

305 of three sub-parameters and the building fabric consists of two sub-parameters. In both cases, the vulnerability rating is calculated as the average ratings of the sub-parameters.

Table 3: Description of each parameter and the vulnerability value allocated for each possible outcome.

Parameter	Sub-parameter	possible outcome	VR	Parameter	Sub-parameter	Possible outcome	VR
1. number of storeys		>=4	100	**7. Building fabric**	frame material	timber	100
		3	70			masonry	55
		2	40			concrete	10
		1	10		wall material	timber	100
2. Footprint		>500	100			masonry	55
		[400, 500)	77.5			concrete	10
		[300, 400)	55	**8. Building condition**		poor	100
		[200, 300)	32.5			good	55
		<200	10			excellent	10
3. Plinth	Height of plinth to road	<-1	100	**9. Surface condition**	vegetation	no	100
		[-1, 0)	77.5			poor	55
		0	55			good	10
		(0, 1]	32.5		inclination	concave	100
		>1	10			flat	55
4. Stilt	Height of stilts	0	100			convex	10
		(0, 0.5)	55		permeability	no	100
		>0.5	10			poor	55
5. Door threshold	door to plinth	0	100			good	10
		(0, 0.1]	70	**10. Drainage system**		no	100
		(0.1, 0.5]	40			poor	55
		>0.5	10			good	10
6. Window sill	window to plinth	0	100	**11. Flood-prevention features**		No	100
		(0, 0.5]	70			Yes	10
		(0.5, 1]	40	***12. traditional construction**		no	
		>1	10			yes	

* factor that used in equation (6)

Hence for each building and for each parameter a vulnerability rating v_{ij}, can be defined, whereby i,

310 ranging from 1 to 163, denotes the building id, and j, ranging from 1 to 11, denotes the parameter under consideration. The vulnerability index VR_i for each building is therefore computed by summation of the vulnerability attribute for each parameter:

$$VR_i = \sum_j v_{ij} \tag{1}$$

The vulnerability rating for each building can range from a minimum of 110 for lowest vulnerability to a maximum of 1100 for the highest vulnerability. To compare the cumulative frequency of each parameter, a normalised vulnerability rating of each parameter nv_{ij} and the total vulnerability index nVR_i was calculated based on Eq(2) and (3).

$$nv_{ij} = \frac{V_{ij} - V_{ij_{min}}}{V_{ij_{max}} - V_{ij_{min}}} \tag{2}$$

$$nVR_i = \frac{VR_i - VR_{i_{min}}}{VR_{i_{max}} - VR_{i_{min}}} \tag{3}$$

To further analyse the data, buildings are grouped in four classes by dividing the vulnerability range in 4 equal parts: Low vulnerability (0.0 to 0.25), Low-medium vulnerability (0.25 to 0.50), medium high (0.50 to 0.75) and high (0.75 to 1.00).

To determine the relative contribution of each parameter to the high and low vulnerability classes rVR_j was calculated based on Eq(4):

$$rVR_j = \frac{\sum_k V_{kj}/k}{\sum_i V_{ij}/i} \tag{4}$$

where j denotes the parameter considered, k denotes the number of buildings in a given vulnerability class and i is the total number of buildings surveyed.

2.6 Economic loss

The computation of the economic losses caused by flood events includes different components, that can be classified as tangible costs, including the physical damage to the building and contents, interruption of work etc.., and other intangible costs, such as loss or damage to objects with sentimental or cultural value, difficult to quantify (Kreibich et al., 2014). The economic loss model proposed in this study considers the physical damage to each building and its content as it can be estimated on the basis of its specific vulnerability (see section 2.5) and a normalised damage factor $D(h_i)$ expressed as a function of the flood depth. Two different damage factors $D_b(h_i)$ and $D_c(h_i)$, for the building and contents, respectively, are used in the present study.

The physical damage to individual buildings can be calculated as the total replacement cost E_i

$$E_i = C(i) * D(h_i) * F_{VR}(VR_i) * A_{Ti} \tag{5}$$

where i indicates the building identifier, C, D, F_{VR} and A_T are the construction cost per unit area of building, the Damage factor, the Vulnerability factor and the surface area of the building directly affected by the flood, respectively. They are derived as follows.

Building cost:

The replacement cost of buildings C(i) includes two parts, the replacement cost of the building $C_B(i)$ and the replacement cost of contents $C_C(i)$.

$$C_B(i) = F_B(i) * F_H(i) * C_0(i) \qquad\qquad (6)$$

where $C_0(i)$ is the estimated construction cost in the study area depending on building type and materials, $F_B(i)$ is a value factor depending on the perceived value of the building, $F_H(i)$ is a value depending on the historic and cultural status of the building. The value factor F_B can be used to account for the depreciated cost, i.e. the current remaining value, rather than the replacement value (Huizinga et al., 2017). However, as several of the buildings in the study area are either historic or traditionally built, neither the depreciated cost or replacement cost might be appropriate to account for their cultural value. ARCADIS (2019) uses a range from 2415 to 4105 RM (525 to 890 €) per square meter to compute the basic construction cost $C_0(i)$ of a detached house in Kuala Lumpur. This value includes the construction and services (electrics, hydraulics and mechanical) costs. In this study the building fabric material (timber, masonry, concrete) is used to determine the low, medium and high cost range, while the building condition (poor, good and excellent) is used to determine the values of the adjustment factor $F_B = (0.4, 0.7, 1)$, respectively. If the building is among the ones identified as of traditional construction by Ju et al. (2012), or listed as of historic value, a factor of $F_H(i) = 1.3$ is applied to account for the additional cultural value as a touristic attraction.

Replacement cost for damage suffered by contents is also a non-negligible component of the total loss suffered by building affected by floods. Huizinga et al. (2017) and FEMA (2013) assume that the replacement cost of content is typically ranging between 40 and 60% for residential properties. However, studies at the microscale (Appelbaum, 1985; Oliveri and Santoro, 2000) show that the proportion of content cost to structure cost also depends on type and quality of construction, level of household income, etc. with a range from 15 to 60 %. Therefore, the content cost can be expressed as:

$$C_C(i) = C_B(i) * k_c$$

where k_c assumes values in the range $(0.15 - 0.60)$, which is also determined according to the building condition in this study.

Finally, combining the building replacement cost $C_B(i)$ and the content replacement cost $C_C(i)$ provides the total replacement cost to buildings. $C(i) = C_B(i) + C_C(i)$

The Flood depth-damage ratio function $D(h_i)$, is a function of the water depth h_i, which in this study is computed as the differential at each building site between the inundation depth computed by the flood hazard model at the road elevation and the elevation of the first floor above ground. The latter is computed as the height of plinth to road + height of stilts + height of door threshold, where the height of plinth to road can be positive or negative.

Depth-damage ratio functions specific for Malaysia or Kuala Lumpur do not exist in literature, as data on losses from past events has not been systematically collected and analysed to date, notwithstanding the frequency of these, even in the last decade (Romali et al., 2018). The derivation of synthetic depth-damage functions relies on appropriate exposure databases, ad-hoc surveys, or heuristic information on losses. When conducting studies at micro scale, as the present one, it is important that the depth-damage ratio function used reflects the damage to single buildings, rather than aggregation at grid cell level or

larger, and also reflect the actual response of the construction to flood. A systematic review of several
385   depth-damage ratio functions produced in literature (Appelbaum, 1985; Dutta et al., 2003; Englhardt et
al., 2019; Huizinga et al., 2017; MLIT, 2005) show the relevance of parameters such as construction
material and quality, number of storeys, conditions, etc, in determining the depth-damage function,
leading to a non-negligible variance among the available functions. However, as the proposed
vulnerability model discussed in section 2 accounts for these characteristics explicitly in the
390   computation of the vulnerability index VR_i for each building, it is appropriate to derive a mean damage
ratio function, only dependent on water depth, while the variance due to the building characteristics are
accounted by the Vulnerability Factor F_{VR} (VR_i) in equation (5). Figure 6 shows the damage ratio
function obtained as regression from the mean values of several damage functions in literature, and the
associated variance for each point in the series. The damage function obtained by regression has a
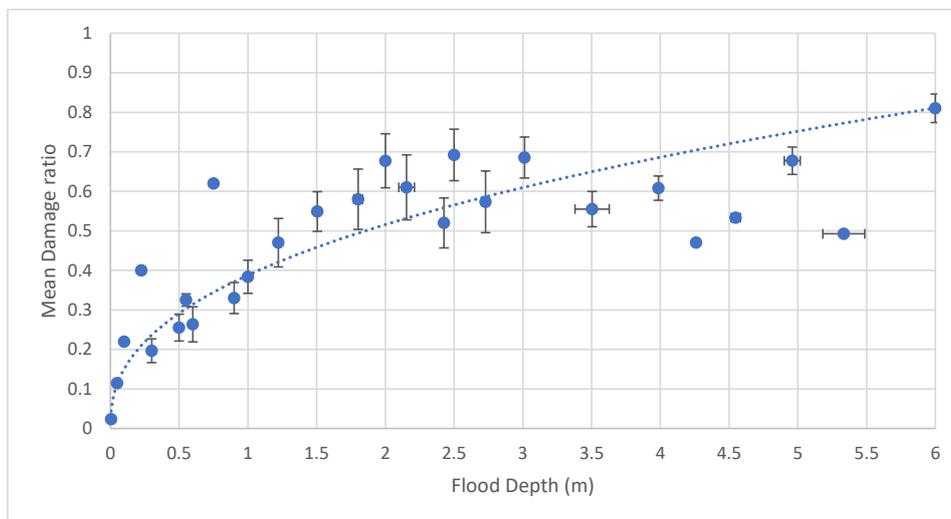395   coefficient of determination $R^2 = 0.846$ (significant at 0.01 level).

Figure 6: Mean damage ratio as function of flood depth with point by point standard deviation.

Vulnerability factor F_{VR}.

400    $$F_{VR}(VR_i) = \frac{VR_i}{VR_{median}}$$ (7)

The vulnerability factor $F_{VR}(VR_i)$ for each building is computed based on the normalised vulnerability
index calculated with equation (1) divided by the median value of the distribution of vulnerability
indexes in the sample of interest. In this way the replacement cost function is calibrated directly on the
local building stock of the study area, while remaining non-dimensional.

405   Total flooded area of each building A_t,
$$A_{Ti} = \sum_{i_f} A_{i_f} * n_{i_f}$$ (8)

15

The total flooded area of each building A_{Ti} equals to the foot print of the buildings A_{i_f} times the number of storey affected by the flood n_{i_f}, which is computed as the integer of the ratio of the flood depth to the building storey height.

410

3. Results

3.1 Vulnerability Index of selected buildings

Based on the empirical model described above, the vulnerability rating VR_j for each parameter were attributed to each building and the total VR_i computed. Figure 7(a) shows that most of the VR_j are normally distributed except the number of storeys, roof height and footprint. As the study area is a relatively small neighbourhood, the type of buildings is relatively uniform, mostly are 2-storey buildings with similar footprint. Nonetheless, the total VR_i shows a Lognormal distribution (Figure 7b), with a coefficient of determination 0.997 (significant at 0.01 level).
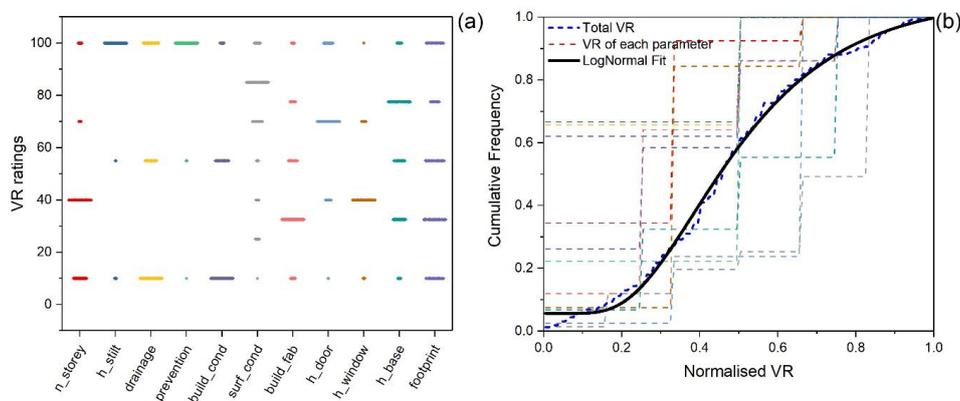
Figure 7: a) Scatter plot of the VR of each parameter b) The cumulative frequency of each parameter and the total VI for the classified sample of buildings.
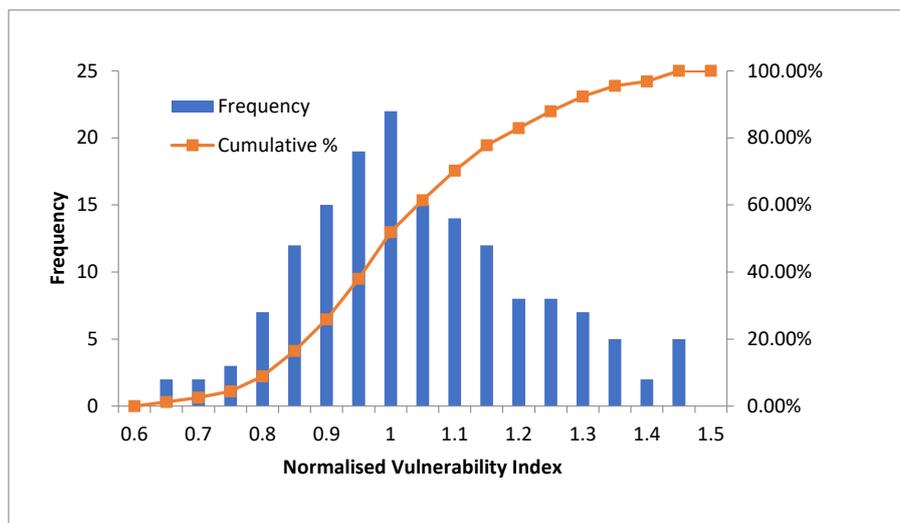
Figure 8: Distribution of normalised vulnerability index VR_i

The largest VR is 852.5, and smallest is 477.5. The distribution of the values normalised with respect
to the median is shown in Figure 8, together with the cumulative density function.

Based on the equal quartile range of the values, the Vulnerability Index range is subdivided in 4 different
categories: low, medium low, medium high, and high, as shown in Table 4. Buildings with medium low
and medium high vulnerability constitute the largest portion of the total 163 buildings surveyed. The
low vulnerability class includes 15% of the sample, while the high vulnerability class includes 13% of
the building. The spatial distribution of the vulnerability index shows a concentration of buildings in
class high vulnerability on the west section of the site, while the central part of the neighbour is
characterised by less vulnerable structures. Nonetheless, the results show that the buildings in the
eastern part of the study area, have higher vulnerability to flooding (Figure 9).

Table 4 Vulnerability Categories and number of buildings in each category

Vulnerability rating	Quartile range values	Percentage of value range	Percentage of sample
Low	477.5-571.25	0%-25%	15
Medium Low	571.25-665	25%-50%	46
Medium High	665-758.75	50%-75%	28
High	758.75-852.5	75%-100%	13

Figure 9: Spatial distribution of VR of each building

3.2 Relevance of factors contributing to vulnerability

Given the apparent random spatial distribution of buildings in the high and low vulnerability categories,
it is worth examining the relevance of the different parameters contributing to the VR_i of each building,
so that the adverse attributes can be mitigated to reduce risk to flood hazards. For buildings in the two
extreme categories of vulnerability, as per eq. 4, the average scoring of each parameter in that category
is divided by the average scoring of the same parameter over the whole sample, hence highlighting the
parameters that most contribute to the low or high vulnerability scoring. This is graphically shown in
Figure 10, where 1 is the normalised value of the mean for each parameter over the whole sample. It is
shown that for the high vulnerability class, poor drainage system, buildings condition and height of base,
all more than 40% larger than the average score, contribute most to high values of VR_i. Conversely,
good drainage system, existence of stilt on the ground to elevate the plinth height, as well as good
building conditions, are key parameters in reducing the vulnerability scoring. This is a relevant finding,
as commonly, for studies at mesoscale, it is assumed that parameters such as drainage and building
conditions can be assumed as uniform over an urban block, for instance. In relation to Kampung Baru
the spatial distribution of the results demonstrates that the provision for drainage might be rather
fragmented, even along the same street, in parts owing to plots redevelopments at different times.

Note that the low vulnerability buildings exhibit the lower vulnerability ratings for most parameters,
except number of storey, which is closely related to the total value exposed to flood hazard. As most
newer buildings have relatively a higher number of storeys, they have higher vulnerability for this
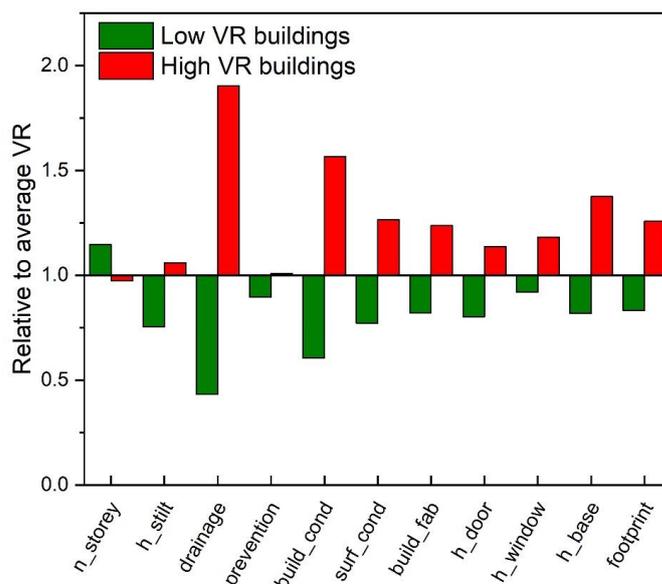parameter while they perform better in relation to other parameters.

Figure 10: Relative values of Low/High VR buildings to the average VR for each parameter
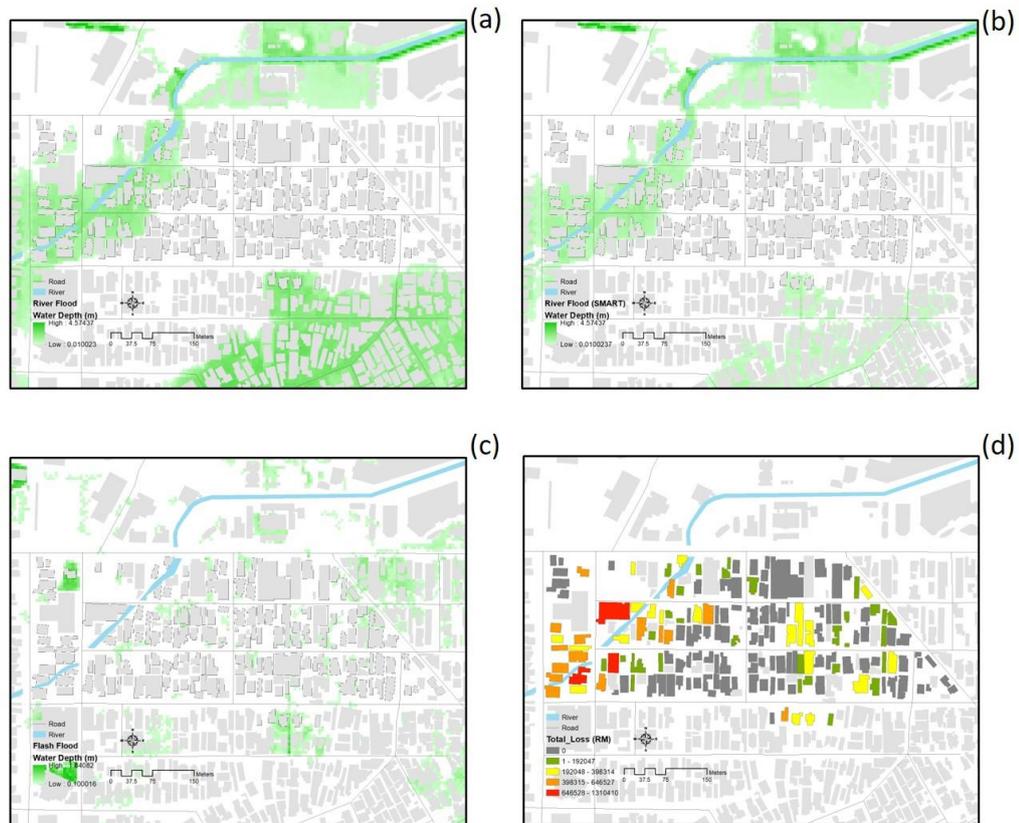
3.3 Estimation of replacement cost due to different flood scenarios

To estimate the flood damage to buildings, as introduced in section 2.2, 3 different scenarios are considered: a pluvial flood, a fluvial flood without structural defences and a fluvial flood considering the effect of the SMART tunnel defence (Abdullah, 2004). For all scenarios the reference rainfall with a 100 years return period is considered here and the extent of flood water for each scenario is presented in Figure 11, together with the total losses (risk map) associated to both fluvial and pluvial events, without the SMART effect. The number of buildings flooded and economic loss as a function of water depth at each building are reported in Figure 12 where the water depth is calculated as the difference between height of stilts and inundation depth, which provides a direct measure of the water depth entering the buildings.

For fluvial flood, the flooded buildings are mostly located in the west part of the study area which is close to Sungai Bunus river. The maximum water depth is around 1.4 m, reducing to less than 1m with the action of SMART. For the pluvial flood, most buildings are flooded to less than 0.2 meter, and have a scattered distribution across the study area. Notwithstanding the differences in depth and spatial distribution of the three scenarios the total number of building flooded varies little, between 20% and 24% of the total building surveyed in the study area (Figure 12a). Note that buildings on the south-east portion of the map, close to Klang river, are also suffering fluvial flood; however, these buildings are outside the area of the present study.

19

the total replacement cost is calculated based on section 2.6. This amounts to around 5M RM for pluvial

flood for the 163 buildings. For river floods, the total cost is considerably higher, around 15M RM

480   without defence and 10M RM with SMART. The percentage of cost to the total replacement cost are

around 1.6%, 4.7%, and 3.1% for pluvial flood , river flood and river flood with SMART respectively.

Major economic loss for fluvial flood are concentrated around 0.2m water depth; for fluvial flood

without SMART Major losses are concentrate in the range between 0.5 to 1.4 m; finally for fluvial

floods with SMART losses are distributed mainly around 0.5m to 0.7 m with a maximum of 1.1.m. We

485   further combine the flood loss due to river flood without SMART (Figure 11a) and flash flood (Figure

11c) to estimate the total flood risk to individual building. The western part of the study area, which is

located at lower topography with Sungai Bunus river passing through, was assessed to have higher risk

to flood.

490   Figure 11: Flood Map of different scenarios (a) River flood without SMART (b) River flood with

SAMRT (c) Flash flood, all on 100 year return period, and (d) estimated total replacement cost due to

river flood without SMART and flash flood
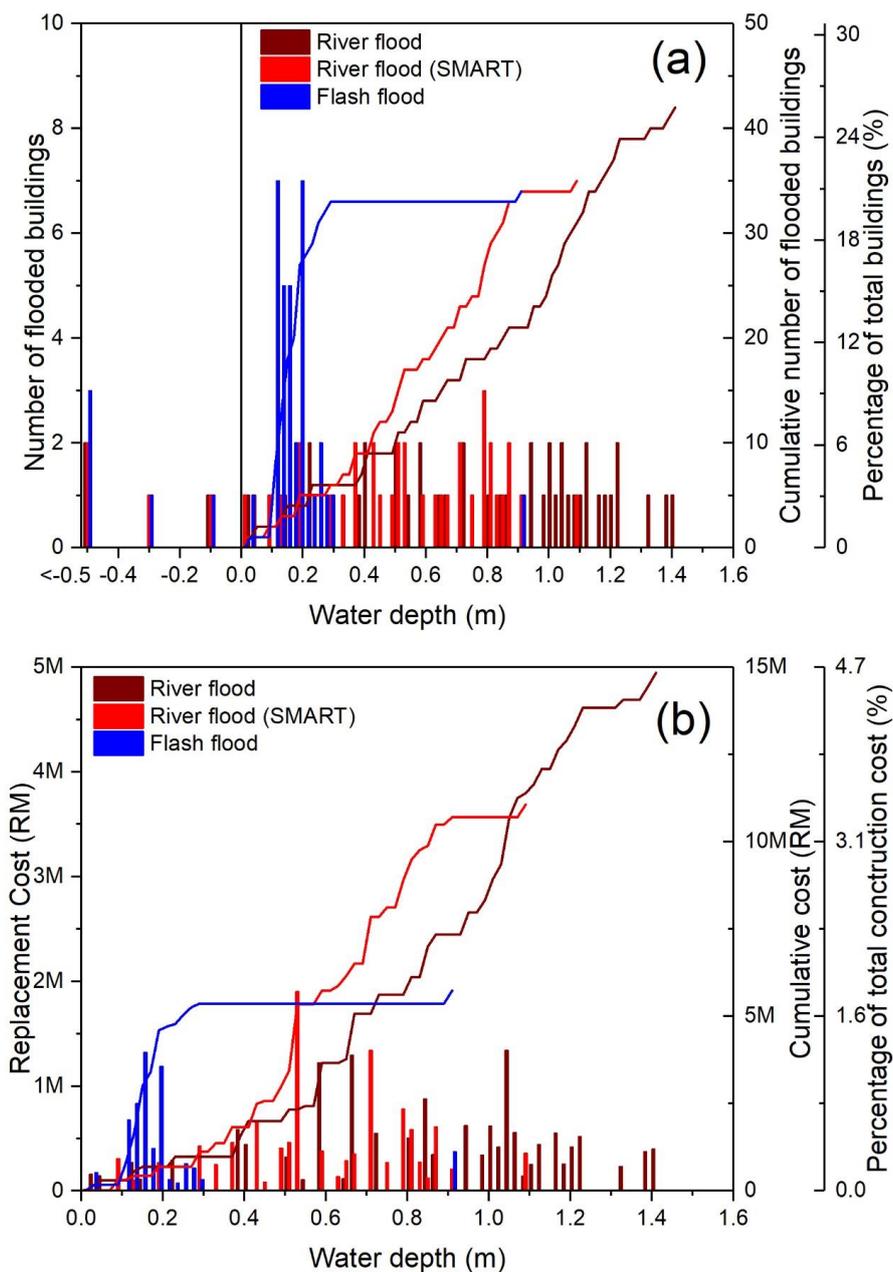
Figure 12: Number of flooded buildings (a) and total replacement cost (b) for different flood scenarios. Some stilted buildings get flooded but have no damage, hence are reported as having negative water depth in (a)

4. Discussion

Flood has become a major hazard worldwide. While major improvements in modelling flood hazard

500 and exposure have been achieved, there is still dearth of compelling evidence on spatio-temporal patterns in vulnerability of societies around the world (Jongman et al., 2015). The Southeast Asian area is more vulnerable due to the higher population density and higher frequency of rainfall. This study focusses on flood vulnerability of the buildings in a small heritage community, Kampung Baru, in the city centre of Kuala Lumpur, Malaysia. This city has experienced an increasing number of flood events

505 due to the combined effects of observed increasing extreme rainfall referred to as Wet Wetter Dry Drier pattern (Allan and Soden, 2008; Allan et al., 2010) as well as an increase of urban population, nearly doubled from 1980 to the current 1.8 million. As the trends for these two variables are not slowing or reversing, it should be expected in the future that both flood hazard and exposure in this city will continue to increase.

510 Buildings, being the primary shelter for people, the reduction of their vulnerability is critical in reducing the risk to flood faced by population. By determining and quantifying the total value of parameters for each building, a classification of vulnerability can be generated in a spatial map to represent how vulnerable each residential building is to flood, thus providing evidence to suggest appropriate design or protection strategies specific to each building in the area. The present study has identified that higher

515 vulnerability is related to absence or poor drainage system, poor building's conditions and poor overall surrounding surface conditions. The buildings with lowest vulnerability show a combination of good drainage systems and surface condition and/or stilts at the ground floor. Thus, several possible solutions can be provided to improve the flood vulnerability of these buildings to reduce the flood risk, among which some feasible strategies are listed below:

520 1.   Increase the ground floor base elevation by either adding pillars or stilts at ground level in new design. The raising floor on stilts is a traditional design of Malaysian vernacular buildings, common of many surveyed cases in Kampong Baru, and such design is being modernised by introduction of open car park at the bottom of high-rise building in Kuala Lumpur. This is considered as a soft measure in the Malaysian national flood prevention programme (DID, 2006). Moreover, as the maximum

525 inundation depth due to flash flood for a 100 year return period is around 0.2m, which is less than the height of most traditional stilts, the stilts are also an effective way to prevent damage from pluvial flood. The present study shows that such strategy can effectively reduce the flood vulnerability and hence risk for individual buildings. However this solution without proper surface treatment and drainage systems may impact adversely neighbouring buildings.

530 2.   'Improving drainage system and surface condition'. Residential buildings which have proper drainage system or vegetation or permeable surrounding ground surfaces or alternatively, set on a higher ground than the road, ensuring a downward slope from the façade to it, were assessed to be in the low

vulnerability class. These conditions are also reflected in the hazard model by varying the % of run off in each grid, although this is at a 5 m resolution. Improved drainage systems are recognised as an

535 efficient way to improve the flood resilience of residential buildings without altering their traditional status. As mentioned above, good drainage is essential for the resilience to extend from the single building to the urban block to the neighbourhood.

3. Finally, the present study also highlights the difference in flood hazard and economic loss between the two fluvial flood scenarios with and without SMART, suggesting that the operation of SMART can

540 reduce the overall flood risk to the study area, although only marginally reducing the number of affected buildings.

Hence a combination of structural measures, e.g. SMART and non-structural measures, e.g. use of stilts and proper surface treatment, appears to be the most effective way to increase the flood resilience from urban scale to building scale.

545 Moreover, major cities in Malaysia such as Kuala Lumpur, Penang, Petaling Jaya and Shah Alam among others have been established floodplains and they are increasingly prone to floods and flash-floods as they develop (Chan, 2011). The use of structural measures is currently under consideration to address the issue of flooding associated with further urban development. The findings from the present study offer decision-makers an option of increasing building scale resilience, to make structural

550 measures more effective. This is particularly relevant in historical cities such as Penang, where traditional Malay buildings are prevalent. The combination of structural and non-structural measures is also in line with the aspirations of civil society groups that seek urban resilience within ecological systems (Connolly, 2019).

5. Conclusions

555 In this study, a localised empirical model has been built to evaluate the flood vulnerability of residential buildings in Kampung Baru, Kuala Lumpur. Combining a field survey, google street view and DEM information, the data of 11 different parameters composing a building level vulnerability model, have been collected and scored to rate the flood vulnerability of a sample of 163 buildings.

The assessed multi-level parameters efficiently represent the vulnerability of residential buildings in the

560 study area. The observed higher flood vulnerability of buildings are closely related to the drainage system and surface condition, as well as the height of the base and condition of the building. Conversely, good drainage system, existence of stilt on the ground to elevate the plinth height, as well as good building conditions, are key parameters in reducing the vulnerability scoring.

A new economic loss model is developed to quantify the flood risk in terms of replacement cost, taking

565 into account both specific vulnerability and a normalised depth-damage ratio function. The function is obtained as regression from the mean values of several damage functions in literatures and is

independent of the specific building typology or local exposure model, which are accounted for in the vulnerability functions. This renders the damage function of generic value and can be applied to other situations in Malaysia and worldwide. The economic loss function considers the loss from both the

570　physical damage to each building and its content. The additional cultural value as a touristic attraction was also calculated as an additional value for the identified traditional buildings. The flood damage and economic loss were then estimated based on the economic loss model under the flood hazards from 3 different scenarios. The western part of the study area, located at a lower topography crossed by the Sungai Bunus river, was assessed to have highest risk to both fluvial and pluvial flood, suggesting that

575　elevation is a major factor at neighbourhood scale. The findings provide multi-scale flood-resistant strategies for the protection of individual residential buildings.

Acknowledgments

Data availability

Building data were collected from a field survey and Google Street View (https://www.google.com/maps/). Primary data are strictly used within the project "Disaster Resilient

585　Cities: Forecasting Local Level Climate Extremes and Physical Hazards for Kuala Lumpur". The data of the research findings are the available from the corresponding author (DDA) on reasonable request.

Author contributions

DDA designed the research and analysed the results; KW and YY collected the data, analysed the results and visualisation; HS, AM and VP conducted the flood modelling; JJP discussed and extended the

590　findings. All authors discussed the results and drafted the final manuscript.

Competing interests

The authors declare that they have no competing interests.

References

Abdullah, K.: Kuala Lumpur: Re-Engineering a Flooded Confluence. Fourteenth Professor Chin Fung
Kee Memorial Lecture. , Kuala Lumpur, Malaysia, 2004.

Aerts, J. C. J. H., Botzen, W. J. W., Emanuel, K., Lin, N., de Moel, H., and Michel-Kerjan, E. O.:
Evaluating Flood Resilience Strategies for Coastal Megacities, Science, 344, 472-474,
10.1126/science.1248222, 2014.

Aliagha, G. U., Iman, A. H. M., Ali, H. M., Kamaruddin, N., and Ali, K. N.: Discriminant factors of
flood insurance demand for flood-hit residential properties: a case for Malaysia, J Flood Risk Manag,
8, 39-51, 10.1111/jfr3.12065, 2015.

Allan, R. P., and Soden, B. J.: Atmospheric warming and the amplification of precipitation extremes,
Science, 321, 1481-1484, 10.1126/science.1160787, 2008.

Allan, R. P., Soden, B. J., John, V. O., Ingram, W., and Good, P.: Current changes in tropical
precipitation, Environ Res Lett, 5, Artn 025205, 10.1088/1748-9326/5/2/025205, 2010.

Amadio, M., Scorzini, A. R., Carisi, F., Essenfelder, A. H., Domeneghetti, A., Mysiak, J., and
Castellarin, A.: Testing empirical and synthetic flood damage models: the case of Italy, Nat. Hazards
Earth Syst. Sci., 19, 661-678, 10.5194/nhess-19-661-2019, 2019.

Appelbaum, S. J.: Determination of Urban Flood Damages, J Water Res Pl-Asce, 111, 269-283, Doi
10.1061/(Asce)0733-9496(1985)111:3(269), 1985.

ARCADIS: Construction Cost Handbook MALAYSIA 2019, Selangor, Malaysia, 2019.

Ashley, R. M., Balmforth, D. J., Saul, A. J., and Blanskby, J. D.: Flooding in the future - predicting
climate change, risks and responses in urban areas, Water Sci Technol, 52, 265-273, 2005.

Balica, S. F., Popescu, I., Beevers, L., and Wright, N. G.: Parametric and physically based modelling
techniques for flood risk and vulnerability assessment: A comparison, Environ Modell Softw, 41, 84-
92, 10.1016/j.envsoft.2012.11.002, 2013.

BERNAMA: Flash flood inundates PKNS shops in Kampung Baru:
http://www.bernama.com/en/news.php?id=1773833, 2019.

Bhuiyan, T., Reza, M., Er, A. C., and Pereira, J.: Direct impact of flash floods in Kuala Lumpur City:
Secondary data-based analysis, ASM Science Journal, 11, 145-157, 2018.

Carisi, F., Schröter, K., Domeneghetti, A., Kreibich, H., and Castellarin, A.: Development and
assessment of uni- and multivariable flood loss models for Emilia-Romagna (Italy), Nat. Hazards Earth
Syst. Sci., 18, 2057-2079, 10.5194/nhess-18-2057-2018, 2018.

CFE-DMHA: Malaysia Disaster Management Reference Handbook 2019, Center for Excellence in
Disaster Management and Humanitarian Assistance, Hawaii, USA, 2019.

Chan, N. W.: Addressing flood hazards via environmental humanities in Malaysia, Malaysian Journal
of Environmental Management, 12, 11-22, 2011.

Chen, A. S., Hammond, M. J., Djordjevie, S., Butler, D., Khan, D. M., and Veerbeek, W.: From hazard
to impact: flood damage assessment tools for mega cities, Nat Hazards, 82, 857-890, 10.1007/s11069-
016-2223-2, 2016.

Connolly, C.: From resilience to multi-species flourishing: (Re)imagining urban-environmental
governance in Penang, Malaysia, Urban Studies, 1-17, 10.1177/0042098018807573, 2019.

Custer, R., and Nishijima, K.: Flood vulnerability assessment of residential buildings by explicit
damage process modelling, Nat Hazards, 78, 461-496, 10.1007/s11069-015-1725-7, 2015.

D'Ayala, D., Galasso, C., Putrino, V., Fanciullacci, D., Barucco, P., Fanciullacci, V., Bronzino, C.,
Zerrudo, E., Manalo, M., Fadriquela, C., Regalado, J., Garciano, L., Oreta, A., and Yu, K. K.:
Assessment of the Multi-Hazard Vulnerability of Priority Cultural Heritage Structures in the Philippines,
1st International Conference on Natural Hazards & Infrastructure, Chania, Greece, 2016,

DID: Guidelines on Flood Loss Prevention Measures for Basement Car Parks Department for Irrigation
and Drainage, Malaysia, 39, 2006.

DID: Managing the Flood Problem in Malaysia, Department for Irrigation and Drainage, Malaysia,
2008.

Dottori, F., Figueiredo, R., Martina, M. L. V., Molinari, D., and Scorzini, A. R.: INSYDE: a synthetic,
probabilistic flood damage model based on explicit cost analysis, Nat Hazard Earth Sys, 16, 2577-2591,
10.5194/nhess-16-2577-2016, 2016.

Dutta, D., Herath, S., and Musiakec, K.: A mathematical model for flood loss estimation, J Hydrol, 277,
24-49, 10.1016/S0022-1694(03)00084-2, 2003.

Englhardt, J., de Moel, H., Huyck, C. K., de Ruiter, M. C., Aerts, J. C. J. H., and Ward, P. J.:
Enhancement of large-scale flood risk assessments using building-material-based vulnerability curves
for an object-based approach in urban and rural areas, Nat. Hazards Earth Syst. Sci., 19, 1703-1722,
10.5194/nhess-19-1703-2019, 2019.

FEMA: Multi-hazard loss estimation methodology HAZUS-MH - Flood Model Technical Manual. ,
Washington, D.C., 569, 2013.

Herbert, D. M., Gardner, D. R., Harbottle, M., and Hughes, T. G.: Performance of single skin masonry
walls subjected to hydraulic loading, Mater Struct, 51, ARTN 97, 10.1617/s11527-018-1222-z, 2018.

Hirabayashi, Y., Mahendran, R., Koirala, S., Konoshima, L., Yamazaki, D., Watanabe, S., Kim, H., and Kanae, S.: Global flood risk under climate change, Nat Clim Change, 3, 816-821, 10.1038/Nclimate1911, 2013.

Huizinga, J., Moel, H. d., and Szewczyk, W.: Global flood depth-damage functions: Methodology and the database with guidelines, Joint Research Centre, European CommissionEUR 28552 EN, 2017.

Inaoka, M., Takeya, K., and Akiyama, S.: JICA's policies, experiences and lessons learned on impacts of urban floods in Asia(*), Int J Water Resour D, 35, 343-362, 10.1080/07900627.2018.1444980, 2019.

IPCC: Climate Change 2013: The Physical Science Basis. Contribution of Working Group I to the Fifth Assessment Report of the Intergovernmental Panel on Climate Change, edited by: Stocker, T. F., Qin, D., Plattner, G.-K., Tignor, M. M. B., Allen, S. K., Boschung, J., Nauels, A., Xia, Y., Bex, V., and Midgley, P. M., Cambridge University Press, Cambridge, United Kingdom and New York, NY, USA, 1535 pp., 2013.

IPCC: Climate Change 2014 – Impacts, Adaptation and Vulnerability: Part A: Global and Sectoral Aspects : Working Group II Contribution to the IPCC Fifth Assessment Report, edited by: Field, C. B., Barros, V. R., Dokken, D. J., Mach, K. J., Mastrandrea, M. D., Bilir, T. E., Chatterjee, M., Ebi, K. L., Estrada, Y. O., Genova, R. C., Girma, B., Kissel, E. S., Levy, A. N., MacCracken, S., Mastrandrea, P. R., and White, L. L., Cambridge University Press, Cambridge, 1140 pp., 2014.

Jacobson, C. R.: Identification and quantification of the hydrological impacts of imperviousness in urban catchments: A review, Journal of Environmental Management, 92, 1438-1448, https://doi.org/10.1016/j.jenvman.2011.01.018, 2011.

Jha, A. K., Bloch, R., Lamond, J., ebrary, I., Bloch, R., Lamond, J., and World, B.: Cities and flooding : a guide to integrated urban flood risk management for the 21st century, World Bank, Washington, D.C, 638 pp., 2012.

Jongman, B., Winsemius, H. C., Aerts, J. C. J. H., Coughlan de Perez, E., van Aalst, M. K., Kron, W., and Ward, P. J.: Declining vulnerability to river floods and the global benefits of adaptation, Proceedings of the National Academy of Sciences, 112, E2271, 10.1073/pnas.1414439112, 2015.

Ju, S. R., Omar, S., and Ko, Y. E.: Modernization of the Vernacular Malay House
 In Kampong Bharu, Kuala Lumpur, Journal of Asian Architecture and Building Engineering, 11, 95-102, 10.3130/jaabe.11.95, 2012.

Kelman, I., and Spence, R.: A limit analysis of unreinforced masonry failing under flood water pressures, Masonry International, 16, 51-61, 2003.

Kreibich, H., van den Bergh, J. C. J. M., Bouwer, L. M., Bubeck, P., Ciavola, P., Green, C., Hallegatte, S., Logar, I., Meyer, V., Schwarze, R., and Thieken, A. H.: Costing natural hazards, Nat Clim Change, 4, 303-306, DOI 10.1038/nclimate2182, 2014.

690 KTA Tenaga Sdn. Bhd.: Flood Damage Assessment Of 26 April 2001 Flooding Affecting the Klang Valley and the Generalised Procedures and Guidelines for Assessment of Flood Damages, Department for Irrigation and Drainage (DID), 2003.

Kundzewicz, Z. W., Kanae, S., Seneviratne, S. I., Handmer, J., Nicholls, N., Peduzzi, P., Mechler, R., Bouwer, L. M., Arnell, N., Mach, K., Muir-Wood, R., Brakenridge, G. R., Kron, W., Benito, G., Honda,
695 Y., Takahashi, K., and Sherstyukov, B.: Flood risk and climate change: global and regional perspectives, Hydrolog Sci J, 59, 1-28, 10.1080/02626667.2013.857411, 2014.

Kundzewicz, Z. W., Su, B. D., Wang, Y. J., Wang, G. J., Wang, G. F., Huang, J. L., and Jiang, T.: Flood risk in a range of spatial perspectives - from global to local scales, Nat Hazard Earth Sys, 19, 1319-1328, 10.5194/nhess-19-1319-2019, 2019.

700 Lamb, R., Crossley, M., and Waller, S.: A fast two-dimensional floodplain inundation model, Proceedings of the Institution of Civil Engineers - Water Management, 162, 363-370, 10.1680/wama.2009.162.6.363, 2009.

Liao, K.-H.: A theory on urban resilience to floods—a basis for alternative planning practices, Ecology and society, 17, 2012.

705 MENON: Thousands caught unawares as 2m-high flash floods hit KL: https://www.thestar.com.my/news/nation/2009/03/04/thousands-caught-unawares-as-2mhigh-flash-floods-hit-kl, 2009.

Merz, B., Kreibich, H., Schwarze, R., and Thieken, A.: Review article 'Assessment of economic flood damage', Nat Hazard Earth Sys, 10, 1697-1724, 10.5194/nhess-10-1697-2010, 2010.

710 Merz, B., Kreibich, H., and Lall, U.: Multi-variate flood damage assessment: a tree-based data-mining approach, Nat. Hazards Earth Syst. Sci., 13, 53-64, 10.5194/nhess-13-53-2013, 2013.

Milanesi, L., Pilotti, M., Belleri, A., Marini, A., and Fuchs, S.: Vulnerability to Flash Floods: A Simplified Structural Model for Masonry Buildings, Water Resour Res, 54, 7177-7197, 10.1029/2018wr022577, 2018.

715 Min, S. K., Zhang, X. B., Zwiers, F. W., and Hegerl, G. C.: Human contribution to more-intense precipitation extremes, Nature, 470, 378-381, 10.1038/nature09763, 2011.

MLIT: Manual for Economic Evaluation of Flood Control Investment (Draft). Ministry of Land, Infrastructure, Transport and Tourism, 69, 2005.

Mohd Anip, M. H., and Osman, S.: Flash Flood Forecasting and Warning in Malaysia, Jakarta,
720   Indonesia, 2017.

Mysiak, J., Surminski, S., Thieken, A., Mechler, R., and Aerts, J.: Brief communication: Sendai
framework for disaster risk reduction – success or warning sign for Paris?, Nat. Hazards Earth Syst.
Sci., 16, 2189-2193, 10.5194/nhess-16-2189-2016, 2016.

Najibi, N., and Deviveni, N.: Recent trends in the frequency and duration of global floods, Earth Syst
725   Dynam, 9, 757-783, 10.5194/esd-9-757-2018, 2018.

Nasiri, H., and Shahmohammadi-Kalalagh, S.: Flood vulnerability index as a knowledge base for flood
risk assessment in urban area, Journal of Novel Applied Science, 2, 269-272, 2013.

Neumann, B., Vafeidis, A. T., Zimmermann, J., and Nicholls, R. J.: Future Coastal Population Growth
and Exposure to Sea-Level Rise and Coastal Flooding - A Global Assessment, Plos One, 10, ARTN
730   e0118571, 10.1371/journal.pone.0118571, 2015.

Oliveri, E., and Santoro, M.: Estimation of urban structural flood damages: the case study of Palermo,
Urban Water, 2, 223-234, https://doi.org/10.1016/S1462-0758(00)00062-5, 2000.

Pall, P., Aina, T., Stone, D. A., Stott, P. A., Nozawa, T., Hilberts, A. G. J., Lohmann, D., and Allen, M.
R.: Anthropogenic greenhouse gas contribution to flood risk in England and Wales in autumn 2000,
735   Nature, 470, 382-385, 10.1038/nature09762, 2011.

Pittore, M., Haas, M., and Megalooikonomou, K. G.: Risk-Oriented, Bottom-Up Modeling of Building
Portfolios With Faceted Taxonomies, Front. Built Environ., 2018,

PreventionWeb: Basic   Country   Statistics   and   Indicators:
https://www.preventionweb.net/countries/mys/data/, 2019.

740   Rehman, S., Sahana, M., Hong, H. Y., Sajjad, H., and Ahmed, B. B.: A systematic review on approaches
and methods used for flood vulnerability assessment: framework for future research, Nat Hazards, 96,
975-998, 10.1007/s11069-018-03567-z, 2019.

Romali, N., Yusop, Z., Sulaiman, M., and Ismail, Z.: Flood risk assessment: A review of flood damage
estimation model for Malaysia, Jurnal Teknologi, 80, 10.11113/jt.v80.11189, 2018.

745   Roslan, R., Omar, R. C., Hara, M., Solemon, B., and Baharuddin, I. N. Z.: Flood insurance rate map for
non-structural mitigation, E3S Web Conf., 76, 2019.

Shafiai, S., and Khalid, M. S.: Flood Disaster Management in Malaysia: A Review of Issues of Flood
Disaster Relief during and Post-Disaster, ISSC 2016 International Conference on Soft Science, 2016,
163-170,

Natural Hazards
and Earth System
Sciences
Discussions

Open Access

EGU

750   Stephenson, V., and D'Ayala, D.: A new approach to flood vulnerability assessment for historic buildings in England, Nat Hazard Earth Sys, 14, 1035-1048, 10.5194/nhess-14-1035-2014, 2014.

Stone, H., D'Ayala, D., and Wilkinson, S.: The use of emerging technology in post-disaster reconnaissance missions, EEFIT Report, 2017.

Stone, H., Putrino, V., and D'Ayala, D.: Earthquake Damage Data Collection Using Omnidirectional
755   Imagery, Frontiers in Built Environment, 4, 51, 2018.

Tullos, D.: How to achieve better flood-risk governance in the United States, P Natl Acad Sci USA, 115, 3731-3734, 10.1073/pnas.1722412115, 2018.

UNISDR: Sendai Framework for Disaster Risk Reduction 2015-2030, 2015.

Vogel, K., Riggelsen, C., Korup, O., and Scherbaum, F.: Bayesian network learning for natural hazard
760   analyses, Nat. Hazards Earth Syst. Sci., 14, 2605-2626, 10.5194/nhess-14-2605-2014, 2014.

Wang, G. L., Wang, D. G., Trenberth, K. E., Erfanian, A., Yu, M., Bosilovich, M. G., and Parr, D. T.: The peak structure and future changes of the relationships between extreme precipitation and temperature, Nat Clim Change, 7, 268-274, 10.1038/Nclimate3239, 2017.